


BRIEF REPORT



## Cdc42 promotes Bgs1 recruitment for septum synthesis and glucanase localization for cell separation during cytokinesis in fission yeast

Udo N. Onwubiko, Julie Rich-Robinson, Rose Albu Mustaf, and Maitreyi E. Das 

Department of Biochemistry & Cellular and Molecular Biology, University of Tennessee, Knoxville, TN, USA

### ABSTRACT

Cytokinesis in fission yeast involves actomyosin ring constriction concurrent to septum synthesis followed by septum digestion resulting in cell separation. A recent report indicates that endocytosis is required for septum synthesis and cell separation. The conserved GTPase Cdc42 is required for membrane trafficking and promotes endocytosis. Cdc42 is activated by Guanine nucleotide exchange factors (GEFs). Cdc42 GEFs have been shown to promote timely initiation of septum synthesis and proper septum morphology. Here we show that Cdc42 promotes the recruitment of the major primary septum synthesizing enzyme Bgs1 and consequent ring constriction. Cdc42 is also required for proper localization of the septum digesting glucanases at the division site. Thus, Cdc42 is required to promote multiple steps during cytokinesis.

### ARTICLE HISTORY

Received 31 August 2019  
Revised 22 December 2019  
Accepted 12 March 2020

### KEYWORDS

GTPase; Cdc42; cytokinesis;  
Bgs1; Eng1; Agn1

### Introduction

Cytokinesis involves the separation of a mother cell into two new daughters. In most eukaryotes with the exception of plant cells, cytokinesis initiates with the assembly of a medially positioned actomyosin ring that constricts in a regulated manner to form the cleavage furrow [1–3]. In the fission yeast *Schizosaccharomyces pombe*, in addition to a medially positioned contractile actomyosin ring, cytokinesis requires the synthesis of a tri-layered cell-wall structure called the division septum [4,5]. The deposition of the septum begins once the assembled ring matures—a time in which a plethora of proteins necessary for cytokinesis get recruited [6–8]. Septum synthesis initiates concomitantly with ring constriction in fission yeast. The division septum consists of a primary septum, synthesized by the linear- $\beta$ -glucan synthase Bgs1, that is sandwiched by secondary septa synthesized mainly by the branched  $\beta$ -glucan synthase Bgs4 [9–11]. In addition the  $\alpha$ -glucan synthase Mok1 is also required for septum formation [12]. Once ring constriction completes, the septum matures, and the primary septum is degraded by digestive enzymes Eng1 and Agn1 to separate the two new daughter cells, thus completing cytokinesis [13,14]. Improper regulation of cytokinesis could result in ploidy defects and non-viable cells.

The small GTPase Cdc42, is a master regulator of cell polarity in fission yeast and other organisms. Cdc42

has been shown to direct actin mediated membrane trafficking [15–18]. Cdc42 is activated at the division site in a sequential manner to promote timely initiation of septum ingression and septum formation [19]. Cdc42 is activated by the Guanidine nucleotide exchange factors (GEFs) Gef1 and Scd1 [20,21]. During cytokinesis, loss of *gef1* delays the initiation of ring constriction and Bgs1 recruitment, while loss of *scd1* results in aberrant septum morphology [19]. It remains unclear however whether these roles are specific to the GEFs or Cdc42 activity. Cdc42 has also been implicated in the specific trafficking of Bgs1 containing vesicles to the sites of polarized growth, although the mechanism is not known [18]. Gef1 has also been shown to promote endocytosis and proper organization of the scaffold protein Cdc15 [22].

In this study, we assess the specific role(s) of Cdc42 during cytokinesis using a temperature sensitive *cdc42* allele, *cdc42-1625* [17,23]. This allele displays reduced Cdc42 levels and a poorly organized cytoskeleton at the restrictive temperature of 36°C, and thus serves as a hypomorphic allele of *cdc42* [23]. Here we find that altering Cdc42 activity disrupted cytokinesis, impaired Bgs1 localization to the division site, and disrupted localization of the septum remodelling enzymes Eng1 and Agn1. Our results define specific roles of Cdc42 during cytokinesis. We show that Cdc42 is required

for ring constriction by ensuring Bgs1 recruitment, and cell separation via directing proper localization of Eng1 and Agn1.

## Results and discussion

### **Cdc42-1625 mutants display similar septation index with *cdc42+* cells**

To investigate the direct role of Cdc42 in cytokinesis we sought to analyse cytokinetic defects in the temperature sensitive mutant *cdc42-1625*. Both *cdc42+* and *cdc42-1625* cells were first grown at the permissive temperature of 25°C, then shifted to the restrictive temperature of 36°C for 4 hours as previously performed [23]. Cells were stained for cell-wall deposition with calcofluor white, and imaged immediately. *cdc42-1625* mutants appeared wider than *cdc42+* cells even at 25°C, which became further pronounced along with increased cell death at 36°C (Figure 1(a,c)). These observations are consistent with previous reports on the growth defects observed in *cdc42-1625* mutants, even at the permissive temperature of 25°C [23]. We analysed the number of septated cells in 3 replicate experiments, and find an asynchronous population of *cdc42+* cells displayed an average septation index of ~17% at 25°C, and ~15% at 36°C, while *cdc42-1625* strains had septation indices of ~22% at 25°C and ~23% at 36°C (Figure 1(b)). The minor differences in septation indices are not statistically significant (Figure 1(b)). This suggested one of two things, either Cdc42 has no role in cytokinesis, or possibly that septum formation itself is disrupted in the *cdc42-1625* mutant, and thus not detected by analysis of the septation index. The latter seems plausible, given that the Cdc42 GEF Gef1 promotes timely initiation of septum ingression. To test this hypothesis, we assessed septation index in a synchronized population *cdc42+* and *cdc42-1625* cells. Cell cycle block in S-phase was induced by treating cells with 10 mM Hydroxyurea for 4hrs at 25°C [24]. Entry into mitosis occurred at ~100 minutes after drug washout, and this represents  $t = 0$  hr, at which septation index was lowest in all strains (Figure 1(d)). Cells were then shifted to 36°C, and imaged every hour for 4 consecutive hours. Analysis of the septation index in synchronized cells showed that all strains displayed an initial peak in septation after entry into mitosis (Figure 1(d,e)). While *cdc42+* cells at 36°C displayed periodic increases and decreases in the percentage of septated cells through the 4 hour period (Figure 1(d)), *cdc42-1625* cells did not show periodic changes, rather the septation index remained high (Figure 1(d)). This suggests

that in hypomorphic *cdc42-1625* mutants, cytokinesis is prolonged.

### **Cdc42 is required for Bgs1 recruitment to the medial ring during cytokinesis**

Next, we asked if *cdc42-1625* mutants show defects in the recruitment of the major primary septum synthesizing enzyme Bgs1. Bgs1 is recruited to the division site after ring assembly, during ring maturation [19,25]. We assessed Bgs1 localization in an asynchronous population of *cdc42+* and *cdc42-1625* cells expressing Rlc1-tdTomato as a ring marker, and GFP-Bgs1 (Figure 2(a,b)). We compared GFP-Bgs1 intensity in non-constricting *cdc42+* and *cdc42-1625* cells at 25°C and 36°C. We quantified the fluorescence intensities and find that GFP-Bgs1 fluorescence is significantly reduced in *cdc42-1625* mutants at 25°C ( $p < 0.01$ ) and 36°C ( $p < 0.001$ ), compared to *cdc42+* cells (Figure 2(b)). Thus, we find that irrespective of the shift in temperature, the temperature sensitive mutation is effective enough to impair Bgs1 recruitment. We did not observe any differences in GFP-Bgs1 levels in *cdc42+* cells at 25°C or 36°C (Figure 2(b)). We confirmed that GFP-Bgs1 global levels were not decreased in *cdc42-1625* mutants, compared to *cdc42+* cells (Figure 2(d)). If these mutants show defects in Bgs1 recruitment, we postulated that fewer actomyosin ring containing cells would show Bgs1 at the division site. We assessed the number of cells with actomyosin rings containing Bgs1 in *cdc42+* and *cdc42-1625* cells. We find that ~85% of *cdc42+* cells display actomyosin rings with GFP-Bgs1 at 25°C and 36°C (Figure 2(e)). Interestingly ~89% of *cdc42-1625* cells at 25°C, displayed GFP-Bgs1 containing actomyosin rings, and this value was comparable to *cdc42+* cells at 25°C and 36°C (Figure 2(e)). At 36°C however, the percentage of GFP-Bgs1 containing actomyosin rings was significantly reduced to ~64% in *cdc42-1625* cells. We find that at 36°C, fewer actomyosin rings in *cdc42-1625* cells recruit Bgs1. Cdc42 is therefore required for recruitment of Bgs1 to the division site after ring assembly, which likely enables the timely initiation of ring constriction.

While Bgs1 recruitment is impaired in *cdc42-1625* cells, we still see a subset of these cells able to recruit low levels of GFP-Bgs1, and finally complete cytokinesis. Fewer Bgs1 containing rings, would suggest fewer cells undergoing constriction. To address this, we analysed the percentage of *cdc42-1625* mutants able to initiate successful ring constriction. We find

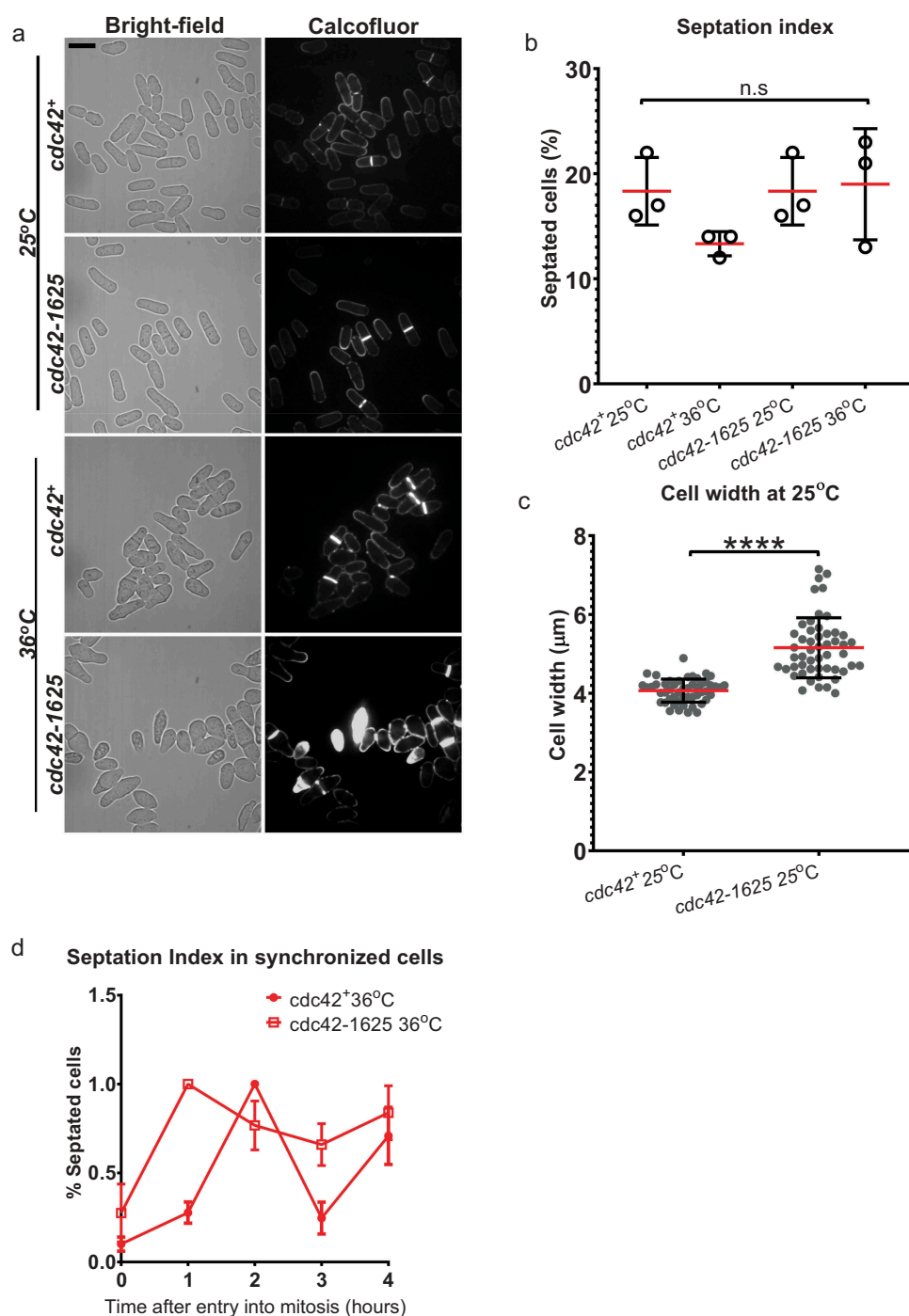


**Figure 1.** *Cdc42-1625* mutants display similar septation index with *cdc42+* cells. (a). Representative images of *cdc42+* and *cdc42-1625* at permissive (25°C) and non-permissive (36°C) temperatures; Scale bar-10 μm. (b). Septation indices for *cdc42+* and *cdc42-1625* at permissive (25°C) and non-permissive (36°C) temperatures, each data point represents an experiment, three replicate experiments were performed. (c). Quantification of cell width in respective strains at permissive temperature (25°C), n = 51 cells. (d). Quantification of septation index in mentioned strains, monitored with calcofluor white hourly for 4 hours in cells synchronized in S-phase with 10 mM Hydroxyurea at 36°C. Septation index at each time point was normalized to the first peak septation index for that strain, n = 3 replicate experiments. The red lines on graph represent the mean; error bars represent standard deviation; statistics is performed with ANOVA, followed by Tukey posthoc analysis, \*\*\*\*P ≤ 0.0001; n.s, not statistically significant.

that of all the actomyosin rings, the percentage of constricting rings in *cdc42+* cells are ~59% at 25°C and 55% at 36°C (figure 2(f)). In *cdc42-1625* mutants, the percentage of constricting rings at 25°C, was 47%,

and this number decreased to 31%, after 4 hours at 36°C (figure 2(f)). Our data therefore indicates that *Cdc42* promotes *Bgs1* recruitment and thus initiation of ring constriction during cytokinesis.

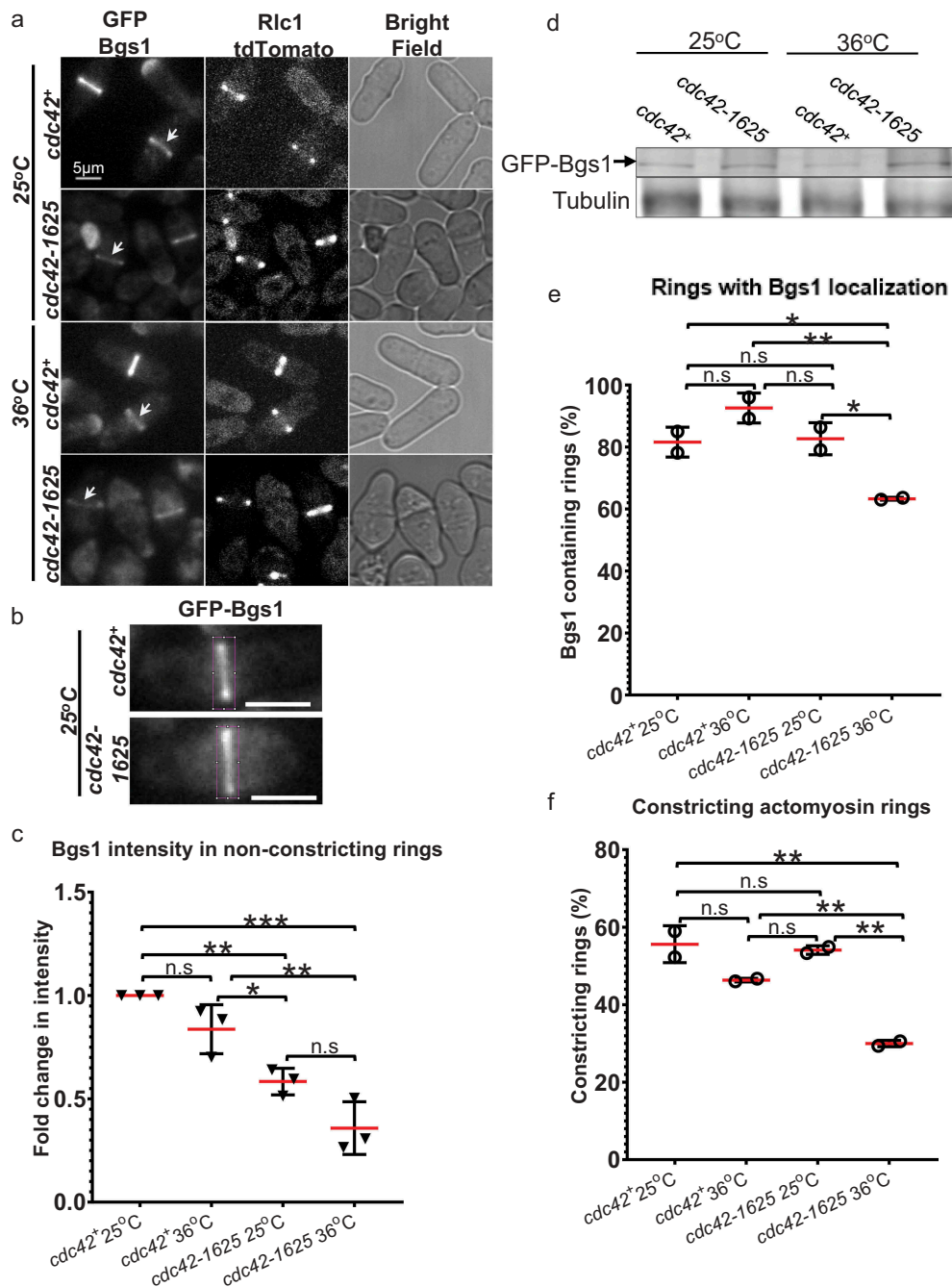


**Figure 2.** Proper Cdc42 function is required for Bgs1 recruitment to the medial ring during cytokinesis. (a). Sum projections showing GFP-Bgs1 and Rlc1-tdTomato localization at permissive (25°C) and non-permissive (36°C) temperatures in *cdc42+* and *cdc42-1625* cells, and respective DIC images. Middle panel shows middle of z-section with Rlc1-tdTomato signal to indicate how we classified non-constricting rings (two distinct dots). The white arrows point to GFP-Bgs1 localization at division site in cells with non-constricting rings. (b). Sum projections of *cdc42+* and *cdc42-1625* cells with magenta box showing 330 pixel<sup>2</sup> box used to measure GFP-Bgs1 signal at the division site. (c). Fold change in GFP-Bgs1 fluorescence intensity, in cells with non-constricting rings in the indicated strains; in comparison to the intensity in *cdc42+* cells at 25°C, n = 3 replicate experiments, with >32 cells for each strain in each experiment. (d). Western Blot showing global GFP-Bgs1 levels at 25°C and 36°C. (e). Quantification of the percentage of cells with rings that display Bgs1 localization, n = 2 replicate experiments, with ≥100 rings analysed per strain. (f). Quantification of the percentage of constricting rings observed among cells with an actomyosin ring in the mentioned strains, at 25°C and 36°C, number of rings analysed (n) ≥100 cells for each strain. The red lines on graph represent mean, error bars represent standard deviation; Statistics is performed with ANOVA, followed by Tukey posthoc analysis, \*P ≤ 0.05; \*\*P ≤ 0.01; \*\*\*P ≤ 0.001; \*\*\*\*P ≤ 0.0001; n.s., not statistically significant; Scale bars- 5 μm.



## **Cdc42 promotes proper localization of digestive enzymes required for cell separation**

While our data indicated that Cdc42 is required for Bgs1 recruitment to the division site, resulting in fewer constricting rings, it fails to explain why the *cdc42-1625* mutants have a septation index similar to the control cells. A previous report suggested that Gef1 has a role in cell separation [26]. Thus, it is possible that the septation index observed in *cdc42-1625* cells is due to a digestion defect of the septa that formed under permissive conditions. To test this, we assessed the role of Cdc42 in septum digestion that leads to cell separation. Cdc42 has also been implicated in endocytosis [22] and polarized trafficking of the exocyst, necessary for proper localization of the digestive enzymes for cell separation [26–28]. To test whether Cdc42 is required for cell separation, we assessed the localization of the digestive glucanases Eng1, and Agn1 which are delivered to the septum during cell separation [13,29]. Eng1-GFP and Agn1-GFP were simultaneously expressed in *cdc42<sup>+</sup>* and *cdc42-1625* strains. Cells were grown at the permissive temperature of 25°C, and imaged to assess Eng1-GFP and Agn1-GFP localization. We observed that these enzymes only localized to septated cells (Figure 3(a)), and there were no obvious differences in the fluorescence intensities in both *cdc42<sup>+</sup>* and *cdc42-1625* cells. Next, we generated 3D-reconstructions of Eng1-GFP Agn1-GFP localization at the division site, to assess localization patterns. We first looked in *cdc42<sup>+</sup>* cells and found three different localization patterns: a ring, a ring and dot, and a disc-like localization (Figure 2(b) (i–iii)). For proper septum digestion these enzymes need to be delivered to the outer rim of the membrane barrier in a ring like pattern [27].

3D-reconstructions of Eng1-GFP Agn1-GFP in *cdc42<sup>+</sup>* cells mainly displayed ‘ring’ and ‘ring and dot’ localization patterns. In *cdc42-1625* mutants at 25 °C, Eng1-GFP Agn1-GFP mostly displayed the ‘disc-like’ pattern (Figure 3(c)), and a ‘ring and dot’ localization that appeared to have larger enzyme deposition in the centre of the ring (Figure 3(c)). The localization of Eng1-GFP Agn1-GFP in *cdc42-1625* cells suggests that these enzymes were not able to localize properly. We quantified the frequency of these patterns within each strain and find that 58% of *cdc42<sup>+</sup>* cells, display rings, 27.3% display a ‘ring +dot’ and 14.3% display ‘disc-like’ localization. In *cdc42-1625* mutants, 1.3% display any rings, 18.3% display a ‘ring +dot’ and 80.3% display ‘disc-like’ localization (Figure 3(d)). We were unable to visualize Eng1-GFP Agn1-GFP localization in cells grown at 36°C for 4hrs. Our results indicate that the localization of the digestive enzymes Eng1 and Agn1 is not polarized, rather appears very diffuse at the division site in *cdc42-1625* cells.

## **Conclusions**

Cytokinesis is a tightly regulated process, and in fission yeast, septum synthesis and ring constriction are properly coordinated to generate viable daughter cells. We report that Cdc42 is required for proper cytokinesis in fission yeast. We have demonstrated that Cdc42 is required for the recruitment of the primary septum synthesizing enzyme Bgs1. Further, we show that Cdc42 is needed for proper spatial localization of the septum digesting glucanases Eng1 and Agn1. Since Cdc42 is an essential protein we used a conditional mutant *cdc42-1625* to investigate its role in cytokinesis. It is possible that Cdc42 has an essential role in cytokinesis and this has not been elucidated to date due to the nature of *cdc42* mutants available. Cdc42 has been reported to play major roles in membrane trafficking events [17,18,22]. It has also been reported that while the Cdc42 GEF Gef1 promotes Bgs1 localization for primary septum synthesis, it is not required for the recruitment of a secondary septum synthesizing enzyme Bgs4 [19]. While the glucanases are mislocalized in *cdc42-1625* mutants, it is unclear what leads to this mislocalization. A possible explanation for this phenotype could be that delays in septum formation and maturation leads to delays in the proper localization of the glucanases. However, given the well-established role of Cdc42 in membrane traffic, it possible that the delivery of the glucanases to the outer rim of the membrane barrier is impaired in these mutants. Thus, it is likely that the role of Cdc42 in cytokinesis is to regulate the recruitment of specific cargo required for distinct steps in cytokinesis. Delivery of Bgs1 and the glucanases occur at spatially distinct regions of the division site. Future research will reveal how Cdc42 promotes precise spatial recruitment of these different enzymes.

## **Materials and methods**

### **Strains and cell culture**

Strains used in this study are listed in Table 1. All *S. pombe* strains used in this study are isogenic to PN972. Unless otherwise mentioned, cells were cultured in yeast extract (YE) medium and grown exponentially at 25°C. Genetic manipulations of strains were carried out using standard techniques [30]. Cells were grown exponentially for at least 3 rounds of eight generations for each assay. On the day of the experiment, cells were grown to O.D. of 0.1 and a subset of control and *cdc42-1625* cell culture was transferred to another flask, and placed in a 36°C shaking incubator for 4 hours before imaging.

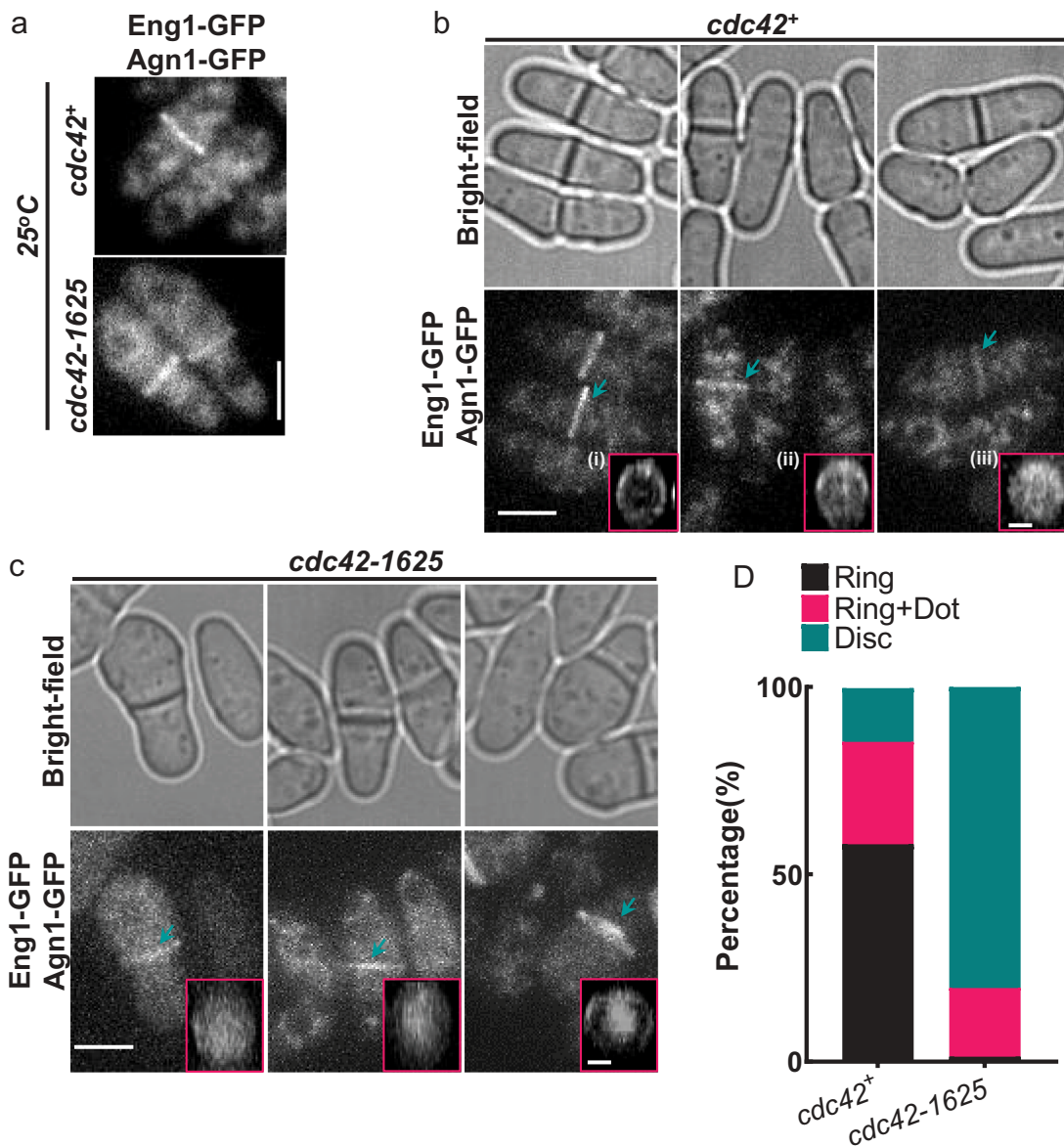


**Figure 3.** Cdc22 is required for proper localization of glucanases Eng1 and Agn1 during cell separation. (a). Sum projections of cells displaying GFP tagged glucanases Eng1 and Agn1 at permissive temperature (25°C) in *cdc42+* and *cdc42-1625* mutants, scale bar-5  $\mu$ m. (b). Representative images showing localization of Eng1-GFP and Agn1-GFP in *cdc42+* cells during cell separation, along with respective bright-field images. The pink boxes highlight the 3D-reconstructions of the different localization patterns of Eng1-GFP and Agn1-GFP observed in *cdc42+* cells: (i) Ring, (ii) Ring + Dot, (iii) Disk. (c). Representative images showing fluorescence images of Eng1-GFP and Agn1-GFP in *cdc42-1625* cells along with the respective bright-field images and 3D-reconstructed division site of Eng1-GFP Agn1-GFP localization during cell separation at 25°C. The pink boxes highlight the 3D-reconstructions of the different localization patterns of Eng1-GFP and Agn1-GFP observed in *cdc42-1625* cells: Scale bar for all cells is 5  $\mu$ m; Scale bar for all 3D-reconstructed division site is 2  $\mu$ m. (d). Quantification of Eng1-GFP and Agn1-GFP localization patterns at the division site in the strains mentioned, n = 3 replicates with  $\leq 28$  cells each.

### Microscopy

Image acquisition was performed at room temperature (23–25°C) with the VT-Hawk 2D- array scanning confocal microscope (Visitech intl., Sunderland, UK) using an Olympus IX-83 inverted microscope with a 100x/numerical aperture 1.49 UAPO lens (Olympus, Tokyo, Japan). Cells were spun down in a mini desk microcentrifuge,

mounted directly onto glass slides with a #1.5 coverslip (Fischer Scientific, Waltham, MA) and imaged promptly. Z-series images were acquired with depth interval of 0.4 $\mu$ m. All Images were acquired with MetaMorph (Molecular Devices, Sunnyvale, CA). All images were analysed with Image J (National Institutes of Health, Bethesda, MD).

**Table 1.** Strains list.

Strain	Genotype	Origin
972	<i>h-</i>	[30]
527	<i>h- ade6-704 leu1-32 ura4-D18 his3-D1</i>	[30]
528	<i>h+ ade6-704 leu1-32 ura4-D18 his3-D1</i>	[30]
PPG5660	<i>h+ cdc42-1625-kanMX leu1-32 ura4-D18</i>	[23]
PPG 3749	<i>h- eng1-GFP KanMX leu1-32 Ura4-D18</i>	[13]
PPG 3781	<i>h- agn1-GFP KanMX leu1-32 Ura4-D18</i>	[29]
YMD825	<i>h+ eng1-GFP-KanMX agn1-GFP-KanMX leu1-34 ura4-D18</i>	This study
YMD1452	$\Delta$ <i>bgs1::ura4 Pbg1::GFP-bgs1:leu1+ rlc1-tdTomato-NAT<sup>r</sup> leu1-32 ura4-D18</i>	This study
YMD 1412	<i>cdc42-1625 GFP-bgs1: leu1 rlc1-tdTomato- NAT<sup>r</sup> leu1-32 ade6-M210 ura4-D18</i>	This study
PPG3750	<i>h- <math>\Delta</math>bgs1::ura4 Pbg1::GFP-bgs1:leu1+ leu1-32 ura4-D18 his3-<math>\Delta</math>1</i>	[31]
YMD1458	<i>cdc42-1625-kanMX eng1-GFP agn1-GFP -KanMX leu1-32 ura4-D18</i>	This study
YMD527	<i>rlc1-tdTomato-NAT<sup>r</sup> ade6-M21X leu1-32 his7 + sad1-mCherry: kanMX ura4-D18</i>	[19]

Statistical analysis was performed using ANOVA, followed by Tukey's HSD Post Hoc Test where appropriate. Comparisons between experimental groups were considered significant when  $p \leq 0.05$ .

### Synchronization of cells using Hydroxyurea

Control and mutant strains were grown for at least 4 generations, and maintained at OD 0.5. On the day of the synchronization, 20mls of cells were grown to an OD of 0.1, and treated with 200ul of 10 mM Hydroxyurea (Sigma H8627, lot# MKCF8706). The treated cells were incubated for 4 hours at 25°C, to synchronize cells in S-phase. At the end of 4hrs, cells were washed 4 times using YE media, and centrifugated at 2000 X g (2 minutes). Cells were then resuspended after final wash in 20 mls of YE. At this stage, synchronization was verified by successful imaging of cells stained with calcofluor via confocal microscopy. Cells were synchronized when at least 80% of cells in the field displayed no septa. 100 mins after drug wash out, a subset of each strain was incubated at the restrictive temperature (36°C). Every hour, 1 ml of cells were concentrated by spinning down, and 2.5ul of cells were mixed with 0.5ul calcofluor and imaged. All Hydroxyurea synchronization experiments were performed in three replicates.

### Calcofluor staining

Cells were grown as described earlier in the methods section, and stained in yeast extract media (YE) with 50  $\mu$ g/ml Calcofluor White (M2 R Sigma-Aldrich, St. Louis, MO) at room temperature. Both controls and mutant strains were washed with fresh YE liquid 1x, and imaged immediately.

### Image analysis

Sum-projections of acquired z-series images were performed in Image J. We quantified GFP-Bgs1 levels from sum-projections of non-constricting cells. Non-constricting cells were judged from the middle z-section, where two adjacent dots of the ring marker Rlc1-Tomato are clearly distinguishable in the cell. Rings are in the constriction stage of cytokinesis if these dots assume the shape of a 'dash' or if these dots have become a solid line at the middle. Next, we measured the intensity at the division site in cells with non-constricting actomyosin rings, using a box with an area of 330 pixel<sup>2</sup>, and reported the integrated density. Background correction was performed with the cytoplasm for each cell.

### Acknowledgments

We thank Pilar Perez and Fred Chang for strains.

### Disclosure statement

No potential conflict of interest was reported by the authors.

### Funding

This work is supported by the National Science foundation (1616495). U.N.O. and J.R.R. were supported by NIH IMSD (R25GM086761) and are currently supported by NSF GRFP (1452154).

### ORCID

Maitreyi E. Das  <http://orcid.org/0000-0001-9164-0158>

### References

- [1] Pollard TD. Mechanics of cytokinesis in eukaryotes. *Curr Opin Cell Biol.* 2010 Feb;22(1):50–56. PubMed PMID: 20031383; PubMed Central PMCID: PMC2871152.
- [2] Li R. Cytokinesis in development and disease: variations on a common theme. *Cell Mol Life Sci.* 2007 Dec;64(23):3044–3058. PubMed PMID: 17882379.
- [3] Guertin DA, Trautmann S, McCollum D. Cytokinesis in eukaryotes. *Microbiol Mol Biol Rev.* 2002 Jun;66(2):155–178. PubMed PMID: 12040122; PubMed Central PMCID: PMC120788.
- [4] Cortes JC, Ramos M, Osumi M, et al. Fission yeast septation. *Commun Integr Biol.* 2016 Jul-Aug;9(4):e1189045. PubMed PMID: 27574536; PubMed Central PMCID: PMC4988442.
- [5] Hercyk BS, Onwubiko UN, Das ME. Coordinating septum formation and the actomyosin ring during cytokinesis in *Schizosaccharomyces pombe*. *Mol Microbiol.* 2019 Dec;112(6):1645–1657. PubMed PMID: 31533197.
- [6] Wu JQ, Kuhn JR, Kovar DR, et al. Spatial and temporal pathway for assembly and constriction of the contractile



- ring in fission yeast cytokinesis. *Dev Cell*. 2003 Nov;5(5):723–734. PubMed PMID: 14602073.
- [7] Roberts-Galbraith RH, Chen JS, Wang J, et al. The SH3 domains of two PCH family members cooperate in assembly of the *Schizosaccharomyces pombe* contractile ring. *J Cell Biol*. 2009 Jan 12;184(1):113–127. PubMed PMID: 19139265; PubMed Central PMCID: PMC2615086.
- [8] Ren L, Willet AH, Roberts-Galbraith RH, et al. The Cdc15 and Imp2 SH3 domains cooperatively scaffold a network of proteins that redundantly ensure efficient cell division in fission yeast. *Mol Biol Cell*. 2015 Jan 15;26(2):256–269. PubMed PMID: 25428987; PubMed Central PMCID: PMCPCMC4294673.
- [9] Cortes JC, Konomi M, Martins IM, et al. The (1,3) beta-D-glucan synthase subunit Bgs1p is responsible for the fission yeast primary septum formation. *Mol Microbiol*. 2007 Jul;65(1):201–217. PubMed PMID: 17581129.
- [10] Munoz J, Cortes JC, Sipiczki M, et al. Extracellular cell wall beta(1,3)glucan is required to couple septation to actomyosin ring contraction. *J Cell Biol*. 2013 Oct 28;203(2):265–282. PubMed PMID: 24165938; PubMed Central PMCID: PMC3812973.
- [11] Cortes JC, Carnero E, Ishiguro J, et al. The novel fission yeast (1,3)beta-D-glucan synthase catalytic subunit Bgs4p is essential during both cytokinesis and polarized growth. *J Cell Sci*. 2005 Jan 1;118(Pt 1):157–174. PubMed PMID: 15615781.
- [12] Garcia Cortes JC, Ramos M, Osumi M, et al. The Cell Biology of Fission Yeast Septation. *Microbiol Mol Biol Rev*. 2016 Sep;80(3):779–791. PubMed PMID: 27466282; PubMed Central PMCID: PMCPCMC4981666.
- [13] Martin-Cuadrado AB, Duenas E, Sipiczki M, et al. The endo-beta-1,3-glucanase eng1p is required for dissolution of the primary septum during cell separation in *Schizosaccharomyces pombe*. *J Cell Sci*. 2003 May 1;116(Pt 9):1689–1698. PubMed PMID: 12665550.
- [14] Dekker N, Speijer D, Grun CH, et al. Role of the alpha-glucanase Agn1p in fission-yeast cell separation. *Mol Biol Cell*. 2004 Aug;15(8):3903–3914. PubMed PMID: 15194814; PubMed Central PMCID: PMCPCMC491845.
- [15] Das M, Verde F. Role of Cdc42 dynamics in the control of fission yeast cell polarization. *Biochem Soc Trans*. 2013 Dec;41(6):1745–1749. PubMed PMID: 24256285.
- [16] Martin SG. Spontaneous cell polarization: feedback control of Cdc42 GTPase breaks cellular symmetry. *Bioessays*. 2015 Nov;37(11):1193–1201. PubMed PMID: 26338468.
- [17] Estravis M, Rincon SA, Santos B, et al. Cdc42 regulates multiple membrane traffic events in fission yeast. *Traffic*. 2011 Dec;12(12):1744–1758. PubMed PMID: 21899677.
- [18] Estravis M, Rincon S, Perez P. Cdc42 regulation of polarized traffic in fission yeast. *Commun Integr Biol*. 2012 Jul 1;5(4):370–373. PubMed PMID: 23060961; PubMed Central PMCID: PMC3460842.
- [19] Wei B, Hercyk BS, Mattson N, et al. Unique spatiotemporal activation pattern of Cdc42 by Gef1 and Scd1 promotes different events during cytokinesis. *Mol Biol Cell*. 2016 Apr 15;27(8):1235–1245. PubMed PMID: 26941334; PubMed Central PMCID: PMCPCMC4831878.
- [20] Coll PM, Trillo Y, Ametzazurra A, et al. Gef1p, a new guanine nucleotide exchange factor for Cdc42p, regulates polarity in *Schizosaccharomyces pombe*. *Mol Biol Cell*. 2003;14(1):313–323. PubMed PMID: 12529446; eng.
- [21] Chang EC, Barr M, Wang Y, et al. Cooperative interaction of *S. pombe* proteins required for mating and morphogenesis. *Cell*. 1994 Oct 7;79(1):131–141. 0092-8674(94)90406-5 [pii]. PubMed PMID: 7923372; eng.
- [22] Onwubiko UN, Mlynarczyk PJ, Wei B, et al. A Cdc42 GEF, Gef1, through endocytosis organizes F-BAR Cdc15 along the actomyosin ring and promotes concentric furrowing. *J Cell Sci*. 2019 Feb 28;132(5):jcs223776. PubMed PMID: 30709916; PubMed Central PMCID: PMCPCMC6432710.
- [23] Martin SG, Rincon SA, Basu R, et al. Regulation of the formin for3p by cdc42p and bud6p. *Mol Biol Cell*. 2007;18(10):4155–4167. PubMed PMID: 17699595; eng.
- [24] Tormos-Perez M, Perez-Hidalgo L, Moreno S. Fission Yeast Cell Cycle Synchronization Methods. *Methods Mol Biol*. 2016;1369:293–308. PubMed PMID: 26519320.
- [25] G. Cortes JC, Ramos M, Konomi M, et al. Specific detection of fission yeast primary septum reveals septum and cleavage furrow ingression during early anaphase independent of mitosis completion. *PLoS Genet*. 2018 May;14(5):e1007388. PubMed PMID: 29813053; PubMed Central PMCID: PMCPCMC5993333.
- [26] Wang N, Wang M, Zhu YH, et al. The Rho-GEF Gef3 interacts with the septin complex and activates the GTPase Rho4 during fission yeast cytokinesis. *Mol Biol Cell*. 2015 Jan 15;26(2):238–255. PubMed PMID: 25411334; PubMed Central PMCID: PMC4294672.
- [27] Martin-Cuadrado AB, Morrell JL, Konomi M, et al. Role of septins and the exocyst complex in the function of hydrolytic enzymes responsible for fission yeast cell separation. *Mol Biol Cell*. 2005 Oct;16(10):4867–4881. E04-12-1114 [pii]. PubMed PMID: 16079182; eng.
- [28] Bendezu FO, Vincenzetti V, Martin SG. Fission yeast Sec3 and Exo70 are transported on actin cables and localize the exocyst complex to cell poles. *PLoS One*. 2012;7(6):e40248. PubMed PMID: 22768263; PubMed Central PMCID: PMC3386988.
- [29] Garcia I, Jimenez D, Martin V, et al. The alpha-glucanase Agn1p is required for cell separation in *Schizosaccharomyces pombe*. *Biol Cell*. 2005 Jul;97(7):569–576. PubMed PMID: 15850449.
- [30] Moreno S, Klar A, Nurse P. Molecular genetic analysis of fission yeast *Schizosaccharomyces pombe*. *Methods Enzymol*. 1991;194:795–823. PubMed PMID: 2005825; eng.
- [31] Cortes JC, Ishiguro J, Duran A, et al. Localization of the (1,3)beta-D-glucan synthase catalytic subunit homologue Bgs1p/Cps1p from fission yeast suggests that it is involved in septation, polarized growth, mating, spore wall formation and spore germination. *J Cell Sci*. 2002 Nov 1;115(Pt 21):4081–4096. PubMed PMID: 12356913.